binding and the behavior of proteins at the membrane surface. Many signal transduction events occur at the cell membrane. For a few well-characterized examples such as Ras and Src, we know that a combination of electrostatic interactions and lipid modifications influence signaling at the membrane [6]. However, there is a growing body of evidence that suggests that the activity of other membrane-associated signaling proteins, including protein kinases, are influenced by voltage changes at the membrane [7, 8]. At first glance, the voltage-dependent differences in stochastic sensing of the interactions between tethered PKIP and PKAc appear to be an unexplained quirky feature of the measurement. Perhaps these unexpected results may lead to powerful new studies to examine the voltage-dependent behavior of proteins kinases and other important signaling molecules at the membrane interface.

The work described above signifies the latest progress in ion channel engineering, a new field which has two major branches. One is devoted to in vivo/therapeutic applications and the other to sensor technology. Recently, engineered channels have been applied to in vivo studies for manipulating electrical excitability in specific neural circuits in transgenic animals [9, 10]. Other work examining expressed engineered channels in cultured neurons in vitro shows that rapid temporal control over the activity of engineered ion channels can be achieved by small chemical ligands or light [11, 12]. These results point to future potential therapeutic applications for engineered ion channels. The use of engineered ion channels as sensors has been in existence for a few years longer. The earliest examples of ion channels as chemical sensors made use of naturally occurring channels. “Patch-cramming,” developed by Richard Kramer, was one notable early example of naturally occurring ion channels used as chemical sensors [13]. The work of Bayley’s group builds on this through the development of engineered channels as specific sensors. To date, virtually all engineered ion channels have been constructed using naturally occurring ion channels as scaffolds. Selection-based membrane protein evolution and de novo design of engineered ion channels are areas that will probably receive substantial attention in the near future. Specifically regarding chemical sensors, there are several challenges that must be solved in order to make channel-based sensors useful as an industrial technology [3]. First, they must be made more physically robust so that they are able to withstand the passage of large volumes of analytes over time. Second, channel-based sensors need to be scaled-up to true multiplex systems to allow for greater throughput. If these technical hurdles can be overcome, then engineered ion channels will likely be directed toward an enormous number of chemical sensing applications.

Todd C. Holmes
Department of Biology
New York University
New York, New York 10003

Selected Reading

1. Xie, H., Bayley, H., Braha, O., Gu, L.-Q., and Cheley, S. (2005). Chem. Biol. *12*, this issue, 109–120.
2. Hladky, S.B., and Haydon, D.A. (1970). Nature *225*, 451–453.
3. Bayley, H., and Jayasinghe, L. (2004). Mol. Membr. Biol. *21*, 209–220.
4. Song, L., Hobaugh, M.R., Shustak, C., Cheley, S., Bayley, H., and Gouaux, J.E. (1996). Science *274*, 1859–1866.
5. Bayley, H., and Cremer, P.S. (2001). Nature *413*, 226–230.
6. Murray, D., Ben-Tal, N., Honig, B., and McLaughlin, S. (1997). Structure *5*, 985–989.
7. Holmes, T.C., Berman, K., Swartz, J.E., Dagan, D., and Levitan, I.B. (1997). J. Neurosci. *17*, 8964–8974.
8. Shen, K., Teruel, M.N., Connor, J.H., Shenolikar, S., and Meyer, T. (2000). Nat. Neurosci. *3*, 881–886.
9. White, B.H., Osterwalder, T.P., Yoon, K.S., Joiner, W.J., Whim, M.D., Kaczmarek, L.K., and Keshishian, H. (2001). Neuron *31*, 699–711.
10. Nitabach, M.N., Blau, J., and Holmes, T.C. (2002). Cell *109*, 485–495.
11. Slimko, E.M., McKinney, S., Anderson, D.J., Davidson, N., and Lester, H.A. (2002). J. Neurosci. *22*, 7373–7379.
12. Banghart, M., Borges, K., Isacoff, E., Trauner, D., and Kramer, R.H. (2004). Nat. Neurosci. *7*, 1381–1386. 10.1038/nn1356
13. Kramer, R.H. (1990). Neuron *4*, 335–341.

Chemistry & Biology, Vol. 12, January, 2005, ©2005 Elsevier Ltd All rights reserved. DOI 10.1016/j.chembiol.2005.01.002

Riboswitch Structures: Purine Ligands Replace Tertiary Contacts

Two recent reports describe the fascinating crystal structures of the G-riboswitch complexed to three different purine ligands, hypoxanthine [1], guanine, and adenine [2].

A riboswitch is a natural RNA biosensor that, in the presence of a specific metabolite, changes conformation, thereby controlling cellular metabolism [3]. Two new studies report three X-ray riboswitch structures: two of the guanine-responsive riboswitch complexed with hypoxanthine at 1.95 Å [1] and guanine at 2.4 Å [2]. The third structure, solved at 2.1 Å resolution [2], is that of the related A-sensing mRNA, in which a single C to U mutation renders the RNA switch adenine specific [4]. In each complex, the RNA has essentially the same length—from 67 to 71 nt. The fold of the RNA fragment is amazingly compact, with a great number of beautifully intricate tertiary interactions. The metabolite is, in each case, sandwiched within a cavity between 4 nucleotides to which it makes specific H bonding contacts. The 5′-UTR of the controlled mRNA exists in a conformational equilibrium between states with or

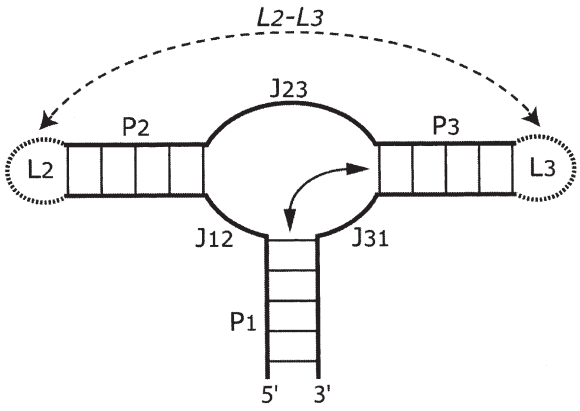

Figure 1. Schematic Drawing of a Three-Way Junction

Schematic drawing of a three-way junction: starting from the 5′ end, Watson-Crick paired stems are numbered P1, P2, P3, with the junctions between them numbered J12, J23, J31 and the capping loops L2 and L3, respectively [2]. When the length of J23 is longer than the other two junction lengths, coaxial stacking between P3 and P1 often occurs (indicated by the continuous double arrows) generally with, depending on the relative lengths of stems P2 and P3 and the fold of J23, loop-loop interactions between the apical loops L2 and L3 (indicated by the dashed double arrows). In such a case, J23 forms a "pseudo-loop" closed by a pair. In the riboswitch, J12, J23, J31 have, respectively, 3, 8, and 2 nucleotides. In the hammerhead ribozymes, the lengths are 2, 7, and 4. For the *Alu* [9] and S [10] domains of the SRP RNA, as well as for the L11 rRNA fragment [8], J12 and J23 are either 0 or 1 with J23 between 4 and 6 nucleotides.

without a transcription terminator helix. The metabolite alters the state of the equilibrium. Interestingly, the similarly bound complexes promote the formation of the terminator helix in the G-riboswitch, thus inactivating transcription, whereas in the A-riboswitch the complex promotes the formation of the antiterminator helix and thus activates transcription [4, 5]. Therefore, positive or negative effects on biological activity can be achieved by the relative position of the riboswitch with respect to neighboring sequences.

Elegantly, Batey and coworkers [1] solved the crystallographic phase problem of the G-riboswitch by using single wavelength anomalous diffraction data on cobalt, while Serganov and coworkers used the anomalous properties of barium for solving the A-riboswitch [2]. The RNA folds are all very similar and, independent of the biological impact of riboswitches recently reviewed [5–7], deserve special focus. Here we will restrict the discussion to the high-resolution G-riboswitch structure complexed with hypoxanthine [1].

At the secondary structure level, the riboswitch forms a three-way junction (Figure 1). This type of junction is frequent in secondary structure diagrams of structured RNAs. For example, ribosomal RNA structures contain several three-way junctions, and a celebrated one is that constituting the L11 protein binding site [8]. The SRP RNA contains two three-way junctions in the Alu and the S domains [9, 10]. With the recent availability of crystallographic structures, some general rules about the folding of RNA three-way junctions start to emerge.

In multiple helical junctions, the choice of coaxial or contiguous stacking of helices is one of the main structural determinants. The junction strands J12, J23, and J31 are rarely of the same length, with one junction strand typically being longer than the other two. In such a case, the coaxial stacking generally occurs opposite to that longer junction strand. Thus, as illustrated in Figure 1, with J23 longer than J12 and J31, helices P3 and P1 will form a contiguous stack. Further, depending on the fold of J23 and the relative lengths of helices P2 and P3, loop-loop interactions between L2 and L3 can form. In all the examples cited above, such loop-loop interactions do occur. The diversity and complexity of those loop-loop tertiary contacts depend on the length of the loops and are astonishing. For example, in the *Alu* domain of the SRP RNA, the loop-loop contacts are essentially made via Watson-Crick pairs [9] while, in the S-domain of the SRP RNA where L2 (capping helix 6) and L3 (capping helix 8) are generally tetraloops, the interactions are made of two consecutive symmetric *trans* pairs involving either the Watson-Crick sites or the sugar-edge sites [10].

The loop-loop interactions in the riboswitch are dominated by two standard Watson-Crick G=C pairs linking the 3′ and 5′ ends of loops L2 and L3, respectively (Figure 2). The sugar-edges of three of the bases involved in the Watson-Crick pairs interact with neighboring adenines, two of which in L3 forming *trans* Hoogsteen/Watson-Crick pairs with bases of L2. Another striking structural feature is the intercalation of an adenine of L2 into L3 forming a *trans* Hoogsteen/Watson-Crick pair below an apical GU platform.

The fold of J23 is a key structural determinant in three-way junctions. In several instances, the first and last residues form a pair, *cis* Watson-Crick in the riboswitch and *trans* Watson-Crick in the L11 rRNA [8] (Figure 3). In two cases (L11 rRNA and the S domain of SRP RNA), the second residue of the "pseudo-loop" forms a U-turn with the next two adjacent adenines involved in A-minor contacts [11, 12] to the last two consecutive canonical Watson-Crick base pairs of P1.

Interestingly, in the riboswitch, two adjacent pyrimidines of J23, following a bulging U and not a U-turn, form *cis* Watson-Crick/sugar-edge pairs with the last two consecutive canonical Watson-Crick base pairs of P1. These interactions constitute a much less frequent minor groove interaction. They all occur within an internal loop, not between distinct RNA elements, and are akin to C motifs [13] (Figure 2). The purine binding site is situated next to those two minor groove contacts, in between J23 and P1, with the Watson-Crick edges of two facing pyrimidines interacting, respectively, with the Watson-Crick and sugar-edge of the purine cofactor (Figure 2). In addition, a standard Watson-Crick base pair links the first residue of J12 with the penultimate residue of J23 and stacks upon the purine cofactor. Finally, the second residue of J12 is engaged in a Watson-Crick/sugar-edge pair with the Watson-Crick pair capping the "pseudo-loop" formed by J23. The purine cofactor, therefore, glues together the P1 helix to the J23 junction and prevents the 3′ strand of the P1 helix to disengage itself and to form alternative structures. The structural comparisons (Figure 2) suggest that the purine cofactor, by mimicking a C-like mo-

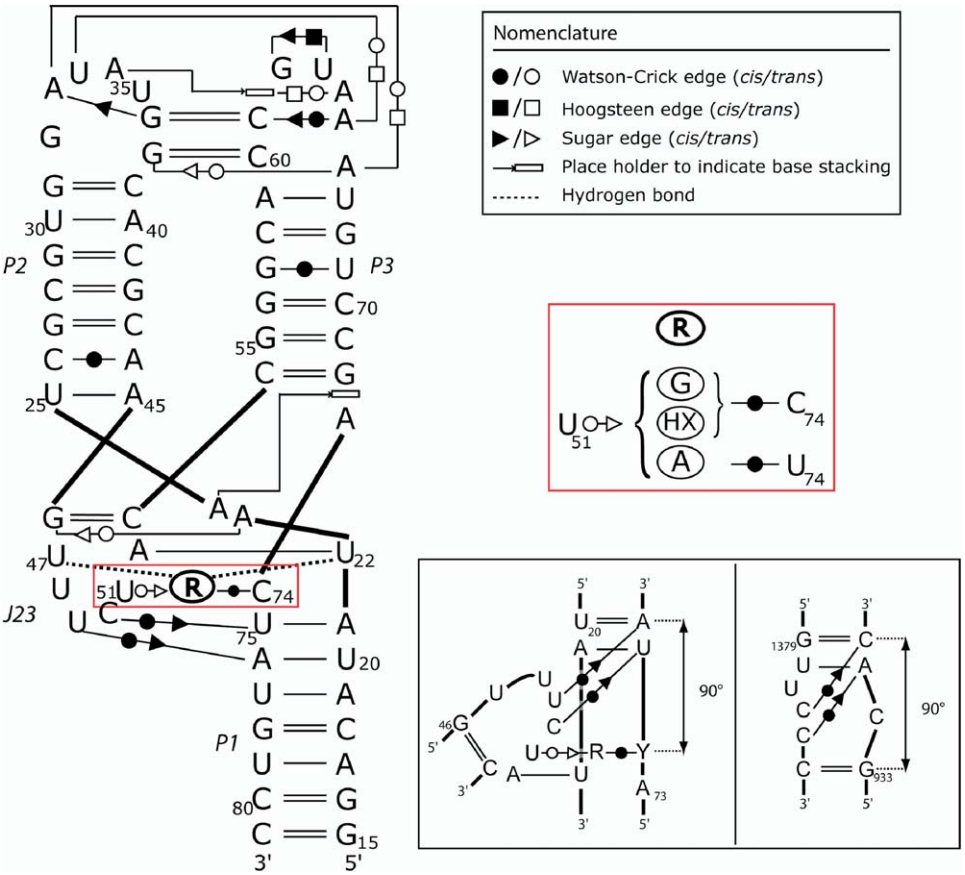

Figure 2. Schematic Representation of the Three-Dimensional X-Ray Structure of the G-Riboswitch Complexed with Hypoxanthine

Schematic representation of the three-dimensional X-ray structure of the G-riboswitch complexed with hypoxanthine [1]. The drawing respects the stacking patterns and illustrates the base edges in contact [17]. A white rectangle indicates in which environment a given base stacks [18]. Minor differences in the base sequence of the helices exist between the three structures [1, 2]. In the middle box, the contacts occurring with the other cofactors are shown following the C to U mutation [2, 4]. It is the pyrimidine interacting with the Watson-Crick edge of the purine cofactor which upon mutation (C to U) changes the purine specificity from G to A. The lower box shows schematic representations illustrating the mimicry between a C-like motif present in helix h28 of the 16S rRNA [13, 19] (at the right) and the purine binding site of the riboswitch [1] (at the left). The riboswitch is made of three strands instead of two as in the h28 internal loop. Two pyrimidines form identical contacts with two consecutive bases engaged in standard Watson-Crick pairs. The R-Y74 Watson-Crick contact is equivalent to the first Watson-Crick pair of the C-like motif. The rotation angles between those first base pairs and the last ones are around 90°.

tif, manages to replace the more frequent and stable double A-minor contacts between the pseudo-loop J23 and the top of helix P1. The mimicry with the C-like motifs is structurally surprising (Figure 2): the rotation angle between the first and the last Watson-Crick pairs of the motif is around 90°, and a similar angle is observed between the equivalent R-Y74 pair and the U20-A76 pair of the riboswitch.

RNA molecules experience a vast range of alternative conformations, extending from a single bulged base occupying various positions within the helical grooves to rearrangements of the secondary and tertiary structures. Riboswitches belong to that class of switchable natural RNA structures [14] which experience a dynamic equilibrium with a definite biological function assigned to it. The first structures of riboswitches represent a major advance toward our understanding of how RNA switches function at the molecular level. This structural knowledge will strengthen the recent progress achieved in molecular engineering of synthetic RNA switches [15] and nanotechnology based on tectoRNA building blocks [16].

Aurélie Lescoute and Eric Westhof
Institut de Biologie Moléculaire et Cellulaire
UPR9002 du CNRS
Université Louis Pasteur
15, rue René Descartes
F-67084 Strasbourg
France

Selected Reading

1. Batey, R.T., Gilbert, S.D., and Montange, R.K. (2004). Nature *432*, 411–415.
2. Serganov, A., Yuan, Y.R., Pikovskaya, O., Polonskaia, A., Malinina, L., Phan, A.T., Hobartner, C., Micura, R., Breaker, R.R., and Patel, D.J. (2004). Chem. Biol. *11*, 1729–1741.
3. Mandal, M., Boese, B., Barrick, J.E., Winkler, W.C., and Breaker, R.R. (2003). Cell *113*, 577–586.
4. Mandal, M., and Breaker, R.R. (2004). Nat. Struct. Mol. Biol. *11*, 29–35.
5. Mandal, M., and Breaker, R.R. (2004). Nat. Rev. Mol. Cell Biol. *5*, 451–463.
6. Nudler, E., and Mironov, A.S. (2004). Trends Biochem. Sci. *29*, 11–17.

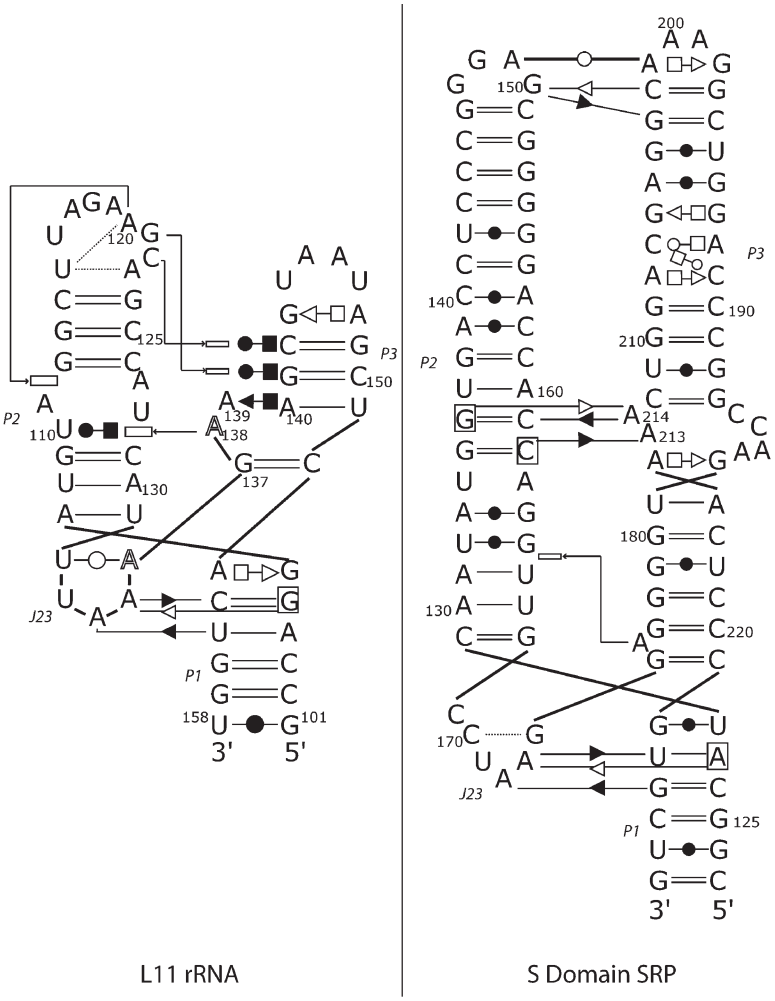

Figure 3. Schematic Representations of the Three-Dimensional X-Ray Structures of the L11 rRNA Complex and the S Domain of the SRP RNA

Schematic representations of the three-dimensional X-ray structures of the L11 rRNA complex (left) [8] and the S domain of the SRP RNA (right) [10]. The drawings follow the same conventions than for Figure 2 and are oriented so as to maximize the similarities between the folds.

7. Winkler, W.C., and Breaker, R.R. (2003). ChemBioChem *4*, 1024–1032.
8. Conn, G.L., Draper, D.E., Lattman, E.E., and Gittis, A.G. (1999). Science *284*, 1171–1174.
9. Weichenrieder, O., Wild, K., Strub, K., and Cusack, S. (2000). Nature *408*, 167–173.
10. Kuglstatter, A., Oubridge, C., and Nagai, K. (2002). Nat. Struct. Biol. *9*, 740–744.
11. Nissen, P., Ippolito, J.A., Ban, N., Moore, P.B., and Steitz, T.A. (2001). Proc. Natl. Acad. Sci. USA *98*, 4899–4903.
12. Doherty, E.A., Batey, R.T., Masquida, B., and Doudna, J.A. (2001). Nat. Struct. Biol. *8*, 339–343.
13. Leontis, N.B., and Westhof, E. (2003). Curr. Opin. Struct. Biol. *13*, 300–308.
14. Silverman, S.K. (2003). RNA *9*, 377–383.
15. Breaker, R.R. (2004). Nature *432*, 838–845.
16. Chworos, A., Severcan, I., Koyfman, A.Y., Weinkam, P., Oroudjev, E., Hansma, H.G., and Jaeger, L. (2004). Science *306*, 2068–2072.
17. Leontis, N.B., and Westhof, E. (2001). RNA *7*, 499–512.
18. Adams, P.L., Stahley, M.R., Gill, M.L., Kosek, A.B., Wang, J., and Strobel, S.A. (2004). RNA *10*, 1867–1887.
19. Brodersen, D.E., Clemons, W.M., Carter, A.P., Wimberly, B.T., and Ramakrishnan, V. (2002). J. Mol. Biol. *316*, 725–768.